

REFERENCE 51

R. GWIN AND D. W. MAGNUSON, "THE MEASUREMENT OF ETA AND OTHER NUCLEAR PROPERTIES OF U²³³ AND U²³⁵ IN CRITICAL AQUEOUS SOLUTIONS," NUCL. SCI. ENG. 12: 364-380 (1962).

NUCLEAR SCIENCE and ENGINEERING

THE JOURNAL OF THE AMERICAN NUCLEAR SOCIETY

EDITOR

EVERITT P. BLIZARD, *Oak Ridge National Laboratory, Oak Ridge, Tennessee*

ASSOCIATE EDITOR

DIXON CALLIHAN, *Oak Ridge National Laboratory, Oak Ridge, Tennessee*

EDITORIAL ADVISORY COMMITTEE

MANSON BENEDICT	O. E. DWYER	RALPH T. OVERMAN
HARVEY BROOKS	PAUL GAST	HUGH C. PAXTON
E. RICHARD COHEN	D. H. GURINSKY	FRANK RING
E. C. CREUTZ	A. F. HENRY	O. C. SIMPSON
W. K. DAVIS	D. G. HURST	B. I. SPINRAD
G. DESSAUER	L. J. KOCH	A. M. WEINBERG
	L. W. NORDHEIM	C. W. J. WENDE

PUBLICATIONS COMMITTEE

J. H. BACH, T. G. LeCLAIR, J. R. LILIENTHAL,
W. E. PARKINS, L. A. TURNER



VOLUME 12, NUMBER 3, MARCH 1962

Copyright© 1962, by American Nuclear Society Inc., Chicago, Ill.

The Measurement of Eta and Other Nuclear Properties of U^{233} and U^{235} in Critical Aqueous Solutions

R. GWIN AND D. W. MAGNUSON

Oak Ridge National Laboratory, Oak Ridge, Tennessee*

Received September 11, 1961

The thermal value of eta for U^{233} and U^{235} has been determined in a series of experiments on unreflected homogeneous aqueous solutions of the two isotopes. These experiments also yield a value for the neutron age and the limiting concentrations of the fissile isotope in the aqueous solutions for infinite volumes. Auxiliary experiments, establishing limits of error, testing certain aspects of the theoretical model employed, and experimentally determining the parameters in the critical equation, have been performed. Experiments performed with 27-in.- and 48-in.-diam spheres, and 5-ft- and 9-ft-diam cylinders have yielded consistent values of eta. Measurements of the nonleakage probability in cylindrical geometry have given values consistent with those predicted by a two-group model in which the theoretical value of the age was used. Within the experimental error no differences were found in the ages of fission neutrons for U^{233} and U^{235} .

The average thermal values of eta determined are: $\bar{\eta}$ for U^{233} , 2.292 ± 0.015 and $\bar{\eta}$ for U^{235} , 2.076 ± 0.015 . The 2200 meters/sec values are the same since the g -factors for eta are unity. The value of the neutron age to the indium resonance energy for U^{235} fission neutrons in water was found to be 25.6 ± 1.3 cm². The minimum U^{233} and U^{235} critical densities for these nitrate solutions were found to be 11.25 ± 0.10 gm/liter and 12.30 ± 0.10 gm/liter for U^{233} and U^{235} , respectively.

INTRODUCTION

A series of experiments has been performed to determine the critical conditions of unreflected homogeneous aqueous uranyl nitrate solutions of both U^{233} and U^{235} . The primary goal of these experiments was to establish the thermal-energy value of eta, $\bar{\eta}$, the number of fission neutrons produced per thermal neutron absorbed in the fissile isotope. In pursuing this goal, it became apparent that a satisfactory conclusion required some experimental confirmation of the theoretical model used for these critical systems. In particular, it was deemed necessary to investigate the applicability of the first fundamental theorem of reactor theory which states that the spatial distribution of neutrons is independent of energy.

The following topics were investigated in the present program:

1. *Critical Parameters.* Critical dimensions of both spherical and cylindrical volumes were measured as a function of the chemical concentration of the fissile

isotope. In one of the spheres, the critical concentration was measured as a function of boron concentration.

2. *Spatial Neutron Flux Distributions.* Flux traverses were made in order to define the buckling, B^2 , or the shape of the neutron flux in these systems from which an extrapolation distance could be obtained.

3. *Kinetic Behavior.* The stable period resulting from an incremental addition of solution to a critical cylinder was measured to determine experimentally nonleakage probabilities and provide some information on the neutron age in these solutions.

4. *Neutron Energy Distributions.* Fission foil activations and fission counting rates were measured using both fissile isotopes as detectors with and without cadmium covers so that corrections could be applied for the epithermal fissions and absorptions in integral form.

5. *Theoretical Analysis.* These experiments have been supported by theoretical investigations of the first fundamental theorem using the "Corn Pone" code (1). Detailed calculations have been made of

* Operated by Union Carbide Corporation for the U.S. Atomic Energy Commission.

the 32-energy group fluxes for the no-return current boundary condition in a 69.2-cm-diam sphere where the leakage of neutrons was great enough to be significant.

These programs have been carried out in a manner such that a limit of error has been placed upon the thermal value of eta.

The initial part of this program, comparing critical concentrations of U²³³ and U²³⁵ in spherical volumes of aqueous solutions, was directed toward the determination of the ratio of the values of eta of the two isotopes, $\bar{\eta}(U^{233})/\bar{\eta}(U^{235})$. In these experiments, which were similar to earlier ones carried out by Thomas *et al.* (2), larger spheres, and thus more dilute solutions, were used in order to reduce the number of epithermal fissions and absorptions and to minimize uncertainties in evaluating the neutron leakage. Cylindrical geometry was chosen for the remainder of the experiments to enable measurement of the nonleakage probability, thus reducing the uncertainties in the derived values of eta. The ages of fission neutrons from U²³³ and U²³⁵ can also be evaluated from the nonleakage probabilities.

In order to utilize these experimental data in determining eta, known cross sections must be used, appropriately evaluated over the neutron spectrum. In effect, then, these critical experiments serve to correlate values of eta, absorption cross sections of the fissile isotopes, and calculated values of the nonleakage probability, and from the latter they yield a value for the neutron age in these solutions.

THEORETICAL CONSIDERATIONS

CRITICAL EQUATION

The theoretical analysis of these chain reacting homogeneous water-moderated assemblies is based upon the theory presented by Weinberg and Wigner (3). Since an extension of this theory using a measured slowing-down kernel with consideration of epithermal absorption has been presented previously (4) only a brief outline of the theory is presented here, beginning with two basic theorems.

The first fundamental theorem of reactor theory states that the stationary neutron distribution $\Phi(\mathbf{x}, E)$ in a critical reactor with energy independent extrapolation distance is separable in space and energy, i.e.,

$$\Phi(\mathbf{x}, E) = \phi(E)\psi(\mathbf{x}) \quad (1)$$

where the spatial distribution, $\psi(\mathbf{x})$, is the fundamental solution of the equation,

$$\nabla^2\psi(\mathbf{x}) + B^2\psi(\mathbf{x}) = 0 \quad (2)$$

that is, that solution which is positive throughout the reactor and vanishes on the extrapolated boundary.

If the neutron flux satisfies Eq. (2) and if the point slowing-down kernel is an isotropic displacement kernel, then the second fundamental theorem of reactor theory states that the nonescape probability of neutrons during moderation in a uniform bare reactor is the Fourier transform of the slowing-down kernel. Since the slowing-down kernel in a bare reactor will change in form near the boundary, the theory cannot be expected to give a detailed description of the neutron flux as a function of position and energy near the boundary. If, except for the region near the boundary, the fluxes at all energies do have the same spatial distribution, then it is possible to formulate the critical conditions for that reactor using these fundamental theorems.

The above concepts lead to the following equation for the balance of neutrons in the thermal energy group, assuming no absorption over the fission spectrum:

$$-\bar{D}B^2\psi(\mathbf{x}) - \bar{\Sigma}_{at}\psi(\mathbf{x}) + K(B, E_{th})p(E_{th})\psi(\mathbf{x}) - \int_0^\infty \phi(E')\Sigma_f(E')\nu(E') dE' = 0 \quad (3)$$

in which an overscore indicates that quantities are averaged over a Maxwellian flux, and

- \bar{D} = diffusion coefficient,
- B^2 = buckling,
- $\bar{\Sigma}_{at}$ = total neutron macroscopic absorption cross section,
- $K(B, E)$ = nonleakage probability during slowing down to energy E ,
- $p(E)$ = probability that a neutron will not be absorbed during slowing down to energy E ,
- $\Sigma_f(E)$ = macroscopic fission cross section at neutron energy E ,
- $\nu(E)$ = average number of neutrons produced per fission by a neutron of energy E .

The spectral distribution of the neutron flux was assumed to be Maxwellian at the system temperature of 24 to 25°C, in the region of thermal energies, supplemented above 0.2 eV by a component very nearly inversely proportional to the energy. The following relations describe this distribution:

$\phi(E) = \phi_M(E) =$ Maxwellian flux for $0 \leq E \leq 0.2$ eV,

$\phi_M(E)$ is normalized so that $\int_0^\infty \phi_M(E) dE = 1$,
 $\phi(E) = \phi_M(E) + [\lambda(E)/E]$ for $0.2 \leq E \leq 10^6$ eV,

$\lambda(E)$ = proportionality factor normalizing the epithermal flux to the Maxwellian.

The term $\lambda(E)$ is defined by

$$\lambda(E) = \frac{K(B, E)}{\xi \Sigma_t(E)} p(E) \cdot \int_0^\infty \phi(E') \Sigma_t(E') \nu(E') dE' \quad (4)$$

in which ξ is the suitably-averaged logarithmic energy decrement and $\Sigma_t(E)$ is the total macroscopic cross section.

The absorption escape probability to thermal energy is:

$$p(E_{th}) = \frac{\int_0^\infty \phi_M(E) \Sigma_{at}(E) dE}{\int_0^\infty \phi_M(E) \Sigma_{at}(E) dE + \int_{0.2}^\infty [\lambda(E)/E] \Sigma_{at}(E) dE} \quad (5)$$

The critical equation used was in the form

$$k_{eff} = \frac{K(B, E_{th})}{1 + L^2 B^2} p(E_{th}) \eta \frac{\bar{\Sigma}_{ax}}{\bar{\Sigma}_{at}} \epsilon = 1 \quad (6)$$

in which $\bar{\Sigma}_{ax}$ is the macroscopic absorption cross section of the fissile isotope, L is the thermal diffusion length, and

$$\epsilon = 1 + \frac{\int_{0.2}^\infty [\lambda(E)/E] \nu(E) \Sigma_t(E) dE}{\eta \bar{\Sigma}_{ax}} = \text{fast fission factor.}$$

By defining:

$$P(B) \equiv \frac{K(B, E_{th})}{1 + L^2 B^2},$$

$$f \equiv \frac{\bar{\Sigma}_{ax}}{\bar{\Sigma}_{at}} = \text{thermal utilization,}$$

and

$$F \equiv \epsilon p(E_{th}),$$

the critical equation becomes:

$$k_{eff} = \eta f F P(B) = k_\infty P(B) = 1. \quad (7)$$

In the above development it is seen that $P(B)$ is the fraction of the source neutrons which do not escape the system. The detailed effect of the absorptions and leakage of epithermal neutrons as a function of energy then appears in the neutron flux, $\lambda(E)/E$. The quantity $K(B, E_{th})$ in the critical equation is the Fourier transform of the point slow-

ing-down kernel to thermal energy. For large systems $B^2 \rightarrow 0$ and $P(B) \rightarrow 1$, eta is equal to $1/f$ except for small corrections due to epithermal neutrons.

EPITHERMAL FLUX PARAMETER

The activations of bare and cadmium-covered fission foils in the critical system, A_{bare} and A_{Cd} , respectively, were used to evaluate the epithermal (>0.4 eV) source of fission neutrons in terms of the total source. The equation used was:

$$\frac{A_{bare}}{A_{Cd}} = \frac{\int_0^\infty \phi_M(E) \Sigma_t dE + \int_{0.2}^\infty \lambda(E) \Sigma_t/E dE}{\int_{0.4}^\infty \lambda(E) \Sigma_t/E dE} \quad (8)$$

The source of neutrons due to fissions induced by neutrons in the energy region between 0.2 and 0.4 eV must be theoretically estimated. The epithermal source permits an average value of λ to be obtained from the expression

$$\lambda \int_{0.4}^\infty \frac{\Sigma_t(E) \nu(E)}{E} dE = \int_{0.4}^\infty \frac{\lambda(E) \Sigma_t(E) \nu(E)}{E} dE. \quad (9)$$

This value of λ , appearing on the left-hand side of the equation, can be applied to the absorption integral within the limits imposed by the assumption that the epithermal flux is proportional to $1/E$, thereby yielding an approximation of the epithermal parasitic neutron capture. The error limits were estimated theoretically to be $\pm 2\%$.

The assumed form of the flux has been compared with those measured by Poole (5) and by Stone and Slovacek (6) in the region where transition from Maxwellian to the $1/E$ distribution occurs. It has been found that the assumed form yields a total U^{235} fission integral which was about 2% lower than that based on the above measured distributions.

NONLEAKAGE PROBABILITY FROM GEOMETRIC BUCKLING PERTURBATIONS

The cylindrical geometry of these experiments permits a change in the buckling of the system by changing the height of the solution of the assembly. This section presents the method used to obtain the nonleakage probability from buckling perturbations. A value of the neutron age can then be obtained from the nonleakage probability. The nonleakage probability during slowing down is given by the Fourier transform of the point slowing-down kernel in an infinite medium. This probability can

be written in moments of r which are defined by the relation

$$\bar{r}^n = \frac{\int_0^\infty G(r)r^n 4\pi r^2 dr}{\int_0^\infty G(r)4\pi r^2 dr} \quad (10)$$

in which $G(r)$ is the slowing-down kernel. The nonleakage probability becomes

$$K(B) = \sum_{i=0}^{\infty} \frac{(-1)^i B^{2i} \bar{r}^{2i}}{(2i+1)!} \quad (11)$$

By using the values of \bar{r}^{2i} calculated by Certain and Aronson (7) for a distribution of fission neutrons in water to indium resonance energy, the nonleakage probability is

$$K(B) = 1 - 25.67B^2 + 815.8B^4 - 3.837 \times 10^4 B^6 + 2.412 \times 10^6 B^8. \quad (12)$$

A representation of $K(B)$ satisfactory to within 0.2% for $B^2 \leq 0.004 \text{ cm}^{-2}$ and satisfactory to within 0.5% for $B^2 \leq 0.007 \text{ cm}^{-2}$ can be written as

$$K(B) = \frac{1}{1 + \tau B^2} \quad \text{where } \tau = 25.67 \text{ cm}^2 \quad (13)$$

This equivalence was used for simplicity in the experimental evaluation of the nonleakage probability described below.

The differential of the critical equation for geometric buckling perturbation is:

$$\Delta k_{\text{eff}} = k_\infty \frac{\partial P(B)}{\partial B^2} \Delta B^2. \quad (14)$$

Further, the kinetic relation connecting the stable reactor period to the change in k_{eff} from unity yields, neglecting the term l/T , which was less than 10^{-6} for this work,

$$\Delta k_{\text{eff}} = k_\infty P_d(B) \sum_i \frac{\beta_i}{1 + \lambda_i T} \quad (15)$$

in which

- β_i = fraction of fission neutrons in the delayed group i ,
- λ_i = decay constant of the i th group of delayed neutrons,
- l = neutron lifetime,
- T = stable reactor period,
- $P_d(B)$ = average nonleakage probability of delayed neutrons.

The nonleakage probability, $P(B_0)$, for a system

having buckling B_0^2 can be obtained by a Taylor's expansion about the nonleakage probability, $P(B)$, for a system having buckling B^2 . In general,

$$P(B_0) = P(B) + \frac{\partial P(B)}{\partial B^2} \Big|_B \Delta B^2 + \frac{\partial^2 P(B)}{(\partial B^2)^2} \Big|_B \frac{(\Delta B^2)^2}{2!} + \dots \quad (16)$$

and since for the infinite system, $P(B_0) = 1$,

$$1 = P(B) + \frac{\partial P(B)}{\partial B^2} \Big|_B (-B^2) + \frac{\partial^2 P(B)}{(\partial B^2)^2} \Big|_B \frac{B^4}{2!} + \dots \quad (17)$$

Using this expansion, the nonleakage probability can be evaluated in terms of its derivatives.

The two-group model, for which

$$P(B) = \frac{1}{(1 + \tau B^2)(1 + L^2 B^2)}, \quad (18)$$

was used to obtain the first and second partial derivatives, and, to terms in B^4 , the nonleakage probability is then

$$P(B) = \frac{1}{2} \left[1 + B^2 \frac{\partial P(B)}{\partial B^2} \right] + \frac{1}{2} \left\{ \left[1 + B^2 \frac{\partial P(B)}{\partial B^2} \right]^2 - 2 \left[B^2 \frac{\partial P(B)}{\partial B^2} \right]^2 A \right\}^{1/2} \quad (19)$$

where

$$A = 1 + \frac{\tau^2}{(1 + \tau B^2)^2} + \frac{L^4}{(1 + L^2 B^2)^2} \cdot \left(\frac{\tau}{1 + \tau B^2} + \frac{L^2}{1 + L^2 B^2} \right)^2. \quad (20)$$

Neglecting terms of higher order than B^4 , $P(B)$ can be written as

$$P(B) = 1 + B^2 \frac{\partial P(B)}{\partial B^2} - \frac{[B^2 \partial P(B) / \partial B^2]^2 A}{2[1 + B^2 \partial P(B) / \partial B^2]} \quad (21)$$

with an error of less than 0.1% provided that B^2 is no greater than 0.004 cm^{-2} .

An interesting relation,

$$S(B) = - \frac{\sum_i \beta_i / (1 + \lambda_i T)}{\Delta B^2} = - \frac{1}{P_d(B)} \cdot \frac{\partial P(B)}{\partial B^2} \quad (22)$$

can be obtained from Eqs. (14) and (15). If

$$P(B) = \frac{1}{\prod_i (1 + L_i^2 B^2)} \quad (23)$$

then

$$\frac{\partial P(B)}{\partial B^2} = -P(B) \sum_i \frac{L_i^2}{1 + L_i^2 B^2} \quad (24)$$

$$S(B) = \frac{P(B)}{P_d(B)} \sum_i \frac{L_i^2}{1 + L_i^2 B^2} \quad (25)$$

and, in the limit of $B^2 = 0$

$$S(0) = -\frac{\partial P(0)}{\partial B^2} = \sum_i L_i^2 = M^2 \quad (26)$$

where M^2 is the migration area of the critical system having zero buckling. Thus $S(B)$ as a function of B^2 yields, as the intercept, the value of M^2 . The age of fission neutrons to thermal energy can, therefore, be obtained from the relation $M^2 = \tau + L^2$.

CALCULATIONS OF STEADY-STATE FLUX DISTRIBUTIONS¹

One of the critical volumes studied experimentally, a 27.24-in.-diam sphere of aqueous solutions of U^{235} was treated analytically using the Corn Pone code (1, 8, 9). Since this volume had the greatest buckling of all those examined in this series of experiments, this particular analysis provides a test of the theoretical model used to analyze the experiments. The calculations yielded the steady-state neutron source and flux as functions of position and energy for various energy groups, with the condition of zero net inwardly directed neutron current at the boundary.

The fluxes and sources in the energy groups were then fitted to the equations

$$\phi(r) = A_\phi \frac{\sin B_\phi r}{B_\phi r} \quad (27)$$

$$S(r) = A_s \frac{\sin B_s r}{B_s r} \quad (28)$$

by a least-squares fit to obtain values of B , the square root of the buckling. These calculations were performed in steps which successively included larger volumes of the sphere until the boundary was reached and show that the departure from the pure $(\sin Br/Br)$ mode is very small. It was observed that the bucklings for the various energy groups were within a range of less than 0.3% when

¹ These calculations were performed by W. E. Kinney using the Corn Pone code on the Oracle.

points within 9 cm of the boundary were omitted; the corresponding value of the extrapolation length, d , is 2.3 cm. The fact that the spatial distribution of neutrons about the center of the reactor is not strongly dependent on their energy is significant in that, for larger systems, there is no reason to expect the effect of the boundary to be projected any further inside the surface than in this case. The application of the fundamental theorems to these large systems is then appropriate. The values of the effective extrapolation length for the source and for the flux of each of various energy groups are shown in Fig. 1. Calculated fluxes over the entire sphere were included in these evaluations. Table I shows the energy corresponding to each of the various groups. Several of the normalized group fluxes are shown in Fig. 2 to illustrate the fact that these fluxes have nearly the same buckling, B^2 .

A calculation was also performed to find the value of B which, when used for all energy groups, gave the same total nonleakage probability as in the previous case. The associated extrapolation distance is 2.4 cm, which compares favorably with the above value of 2.3 cm. However, the assumption of an energy-independent buckling does not describe the detailed leakage in each energy group. In addition, diffusion theory solutions were obtained for the same boundary conditions. A summary of the above calculations is shown in Table II.

EXPERIMENTAL RESULTS

DESCRIPTION OF THE CRITICAL EXPERIMENTS

The critical systems from which data were obtained in these experiments consisted of aqueous solutions of uranyl nitrate enriched in either the U^{233} or the U^{235} isotope. A 27.24-in.-diam aluminum

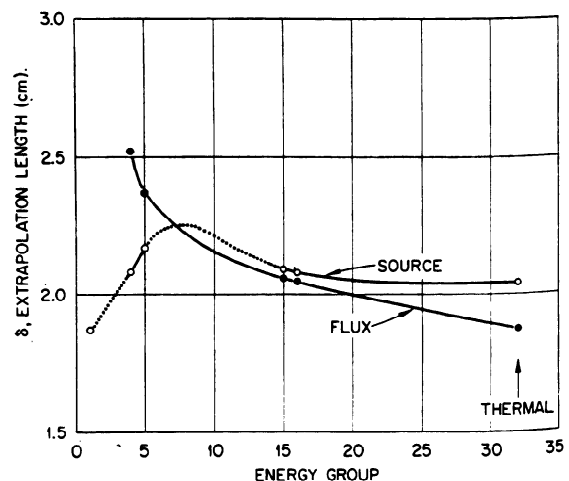
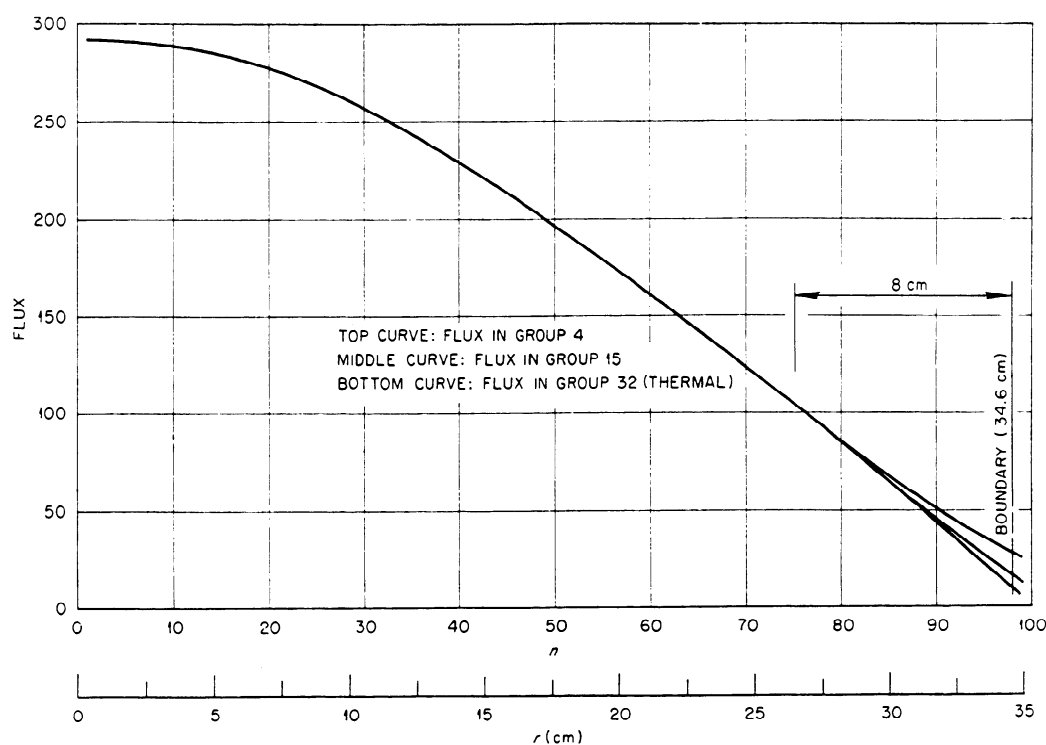


FIG. 1. Extrapolation length as a function of energy group

TABLE I
ENERGY-GROUP LIMITS

Group	Lower energy (ev)	Group	Lower energy (ev)	Group	Lower energy (ev)
	1×10^8	11	3.372×10^1	22	1.523×10^{-1}
1	1×10^7	12	1.515×10^1	23	1.247×10^{-1}
2	6.065×10^6	13	1.016×10^1	24	1.021×10^{-1}
3	3.679×10^6	14	4.564×10^0	25	8.358×10^{-2}
4	2.231×10^6	15	1.375×10^0	26	6.843×10^{-2}
5	1.353×10^6	16	9.214×10^{-1}	27	5.603×10^{-2}
6	8.208×10^5	17	6.176×10^{-1}	28	4.587×10^{-2}
7	1.832×10^5	18	4.140×10^{-1}	29	3.756×10^{-2}
8	9.118×10^3	19	2.775×10^{-1}	30	3.075×10^{-2}
9	4.54×10^2	20	2.272×10^{-1}	31	2.518×10^{-2}
10	1.12×10^2	21	1.860×10^{-1}	32	Thermal

FIG. 2. Flux distributions in a critical sphere ($R = 34.6$ cm) of aqueous U²³³ solution (results of Corn-Pone calculations by W. E. Kinney).

sphere was made critical with both unpoisoned and several boric acid poisoned solutions of both isotopes. A 48.04-in.-diam aluminum sphere was used only with unpoisoned solutions of U²³³ and U²³⁵. A 5-ft-diam stainless steel cylinder, the diameter having been chosen to minimize the buckling for the available amount of U²³³, was made critical at several heights with both U²³³ and U²³⁵. The concluding experiments were performed with U²³⁵ solutions in a 9-ft-diam steel cylinder. At the maximum critical height in this container the neutron leakage was less than 2%, thus limiting the un-

certainty in the value of $\bar{\eta}(U^{235})$ to that resulting from the uncertainty in the cross sections.

BUCKLING MEASUREMENTS AND EXTRAPOLATION DISTANCES

The spatial distribution of neutrons was measured using neutron detectors having different energy responses in order to test the applicability of the first fundamental theorem of reactor theory to these systems. The data from these experiments permit an evaluation of the uncertainty in the derived nonleakage probability introduced by differences of

TABLE II
SUMMARY OF THEORETICAL CALCULATIONS FOR A 34.6-cm-
RADIUS SPHERE^a

Boundary condition ^b	Corn pone		Diffusion theory	
	$P(B)$	k	$P(B)$	k
$j_- = 0$ at $R = 34.6$ cm	0.8374	1.0377	0.8256	1.0231
$\phi = 0$ at $\bar{R} = 35$ cm	0.8212	1.0183	0.8044	0.9977
$\phi = 0$ at $\bar{R} = 36$ cm	0.8297	1.0287	0.8132	1.0086
$\phi = 0$ at $\bar{R} = 37$ cm	0.8375	1.0384	0.8216	1.0189
$\phi = 0$ at $R = 38$ cm	0.8449	1.0475	0.8294	1.0286

^a The calculations were for fuel solutions composed of U^{235} and H_2O only.

^b $\bar{R} = R$ plus the extrapolation length.

the spatial distribution of neutrons near the boundaries of the system. For this purpose flux traverses were taken with U^{238} and cadmium-covered U^{235} miniature counters in addition to the U^{235} miniature counter traverses which were taken in almost all cases.

The normalized counter data were fitted to the form

$$y = \frac{A_\phi \sin B_r(x + x_0)}{B_r(x + x_0)} \quad (29)$$

for spheres, and to the forms

$$y = A_\phi \cos B_h(x + x_0) \quad (30)$$

and

$$y = A_\phi J_0[B_r(x + x_0)] \quad (31)$$

for the height and radius, respectively, of cylinders. The position variable was x , and x_0 was a constant determined by the curve fitting so that the center line positions, $x - x_0$, were zero when the flux had a maximum value.

In a preliminary publication (9) it was reported that analysis of some of these data yielded values of the extrapolation distances for spheres of 1.9 and 1.0 cm. However, it is now believed that these small values were the result of nonideal experimental conditions. Since it was necessary to vary the solution height to maintain criticality as the counter was traversed vertically through the sphere, the solution did not fill the sphere when data were taken in the upper half. The void was greater in the 48-in.-diam sphere, for which d was reported at 1.0 cm. The bucklings calculated from the data of these traverses are not valid even though there were no observable distortions from the expected form of the spatial flux distributions. Values of the extrapolation distances for the experiments in the spheres have been inferred from those obtained from cylinder experiments.

Tables III and IV summarize the buckling values derived from counter traverses in cylindrical systems. The quoted errors are derived from the variances

TABLE III
BUCKLING MEASUREMENTS IN THE 60.92-IN.-DIAM CYLINDER

Detector	Solution height ^a (in.)	(Axial buckling) ^{1/2} , B_h (in. ⁻¹)	Extrapolated height, \bar{h} (in.)	$2d$ (in.)	Extrapolation distance, d (cm)	$B_h^2 \times 10^3$ (cm ⁻²)
U^{235}	18.08	0.1588 ± 0.0006	19.78 ± 0.07	1.70	2.16 ± 0.09	3.909
U^{235}	17.91	0.1588 ± 0.0005	19.78 ± 0.05	1.87	2.37 ± 0.07	3.909
U^{235}	19.08	0.1495 ± 0.0006	21.01 ± 0.08	1.93	2.45 ± 0.10	3.463
$U^{235} + Cd$	19.11	0.1474 ± 0.0005	21.31 ± 0.07	2.20	2.79 ± 0.09	3.367
U^{238}	19.01	0.1469 ± 0.0007	21.39 ± 0.10	2.38	3.02 ± 0.13	3.344
U^{235}	28.81	0.1023 ± 0.00025	30.70 ± 0.08	1.89	2.40 ± 0.10	1.623
U^{235}	42.07	0.0743 ± 0.00012	44.17 ± 0.07	2.10	2.67 ± 0.09	0.784
$U^{235} + Cd$	42.30 ^b min 42.55 ^b max	0.07031 ± 0.00015	44.68 ± 0.09	2.38 2.13	3.02 ± 0.11 2.71 ± 0.11	0.766
U^{238}	42.36	0.07023 ± 0.00045	44.74 ± 0.29	2.38	3.02 ± 0.37	0.764
U^{235}	80.12	0.03805 ± 0.00011	82.57 ± 0.24	2.45	3.11 ± 0.30	0.224

Detector	Height (in.)	(Radial buckling) ^{1/2} , B_r (in. ⁻¹)	Extrapolated radius, \bar{R} (in.)	$d + \Delta R^c$ (in.)	d (cm)	$B_r^2 \times 10^3$ (cm ⁻²)
U^{235}	41	0.07547 ± 0.00020	31.87 ± 0.08	1.41	3.25 ± 0.20	0.883
U^{238}	41	0.07546 ± 0.00034	31.87 ± 0.14	1.41	3.25 ± 0.36	0.883
U^{235}	80	0.07578 ± 0.00018	31.74 ± 0.08	1.28	2.92 ± 0.20	0.890

^a Height measurements have been corrected for bottom reflector (0.53 in.), measured by adding a top constructed like the bottom.

^b Height was varied in order to maintain criticality, the maximum occurring while counter was at center.

^c The correction, ΔR , for the container was assumed to be the wall thickness, 0.13 in. of stainless steel.

TABLE IV
BUCKLING MEASUREMENTS IN THE 107.7-IN.-DIAM CYLINDER

Detector	Solution height ^a (in.)	$\bar{h} - h_c$ (in.)	$B_k^2 \times 10^3$ (cm ⁻²)
Gold	35.78	3.17 ± 0.08	1.008
U ²³⁵	35.78	2.96 ± 0.11	1.020
U ²³⁵	35.78	2.92 ± 0.18	1.021
U ²³⁵	35.68	2.95 ± 0.08	1.025
U ²³⁵	48.47	1.81 ± 0.19	0.605
U ²³⁵	48.54	2.26 ± 0.20	0.592
U ²³⁵	91.43	3.48 ± 0.14	0.170

Detector	Solution height	$\bar{R} - R_c$	$B_k^2 \times 10^3$ (cm ⁻²)
U ²³⁵	35.78	1.90 ± 0.15	0.288
U ²³⁵	91.59	1.92 ± 0.11	0.288

^a The values of the solution dimensions have not been corrected for effects due to structure surrounding the critical cylinder of solution. The difference in column 3 is, therefore, not exactly proportional to the extrapolation distance.

calculated in the curve fitting of the experimental data. Counter data taken within 2 in. of the boundary were excluded from the analyses. A number of flux traverses were also analyzed excluding data at a greater distance from the boundaries, and the derived B values, although slightly different, reflected only errors of measurements and not a variation in curvature with distance from center. The errors associated with the data points near the boundary were no larger than the errors of the other data. Although the counting errors in any particular traverse show no difference between different-sized systems, the derived values of the extrapolation distance in the 5-ft-diam cylinder were internally more consistent than those made in the 9-ft-diam cylinder. It is believed that inaccuracies in height measurements in the latter cylinder are responsible. When the extrapolation distances are plotted for different critical heights in the 5-ft cylinder, a variation greater than their errors is noted. However, it is only for the 27.24-in.-diam sphere and the short cylinders that this variation of d , ~0.8 cm, can affect the nonleakage probability by as much as 0.5%. Figure 3 shows this variation.

The extrapolation distances measured with U²³⁵ fast-neutron detectors showed no variation with critical height greater than the experimental error, the average value being 3.02 ± 0.28 cm. The average value of the epithermal extrapolation distance, measured with cadmium-covered U²³⁵ detectors, was 2.84 ± 0.15 cm. Fast and epithermal measurements were made at critical heights of 18 and 41 in. in the 5-ft-diam cylinder.

The apparent difference between the thermal and

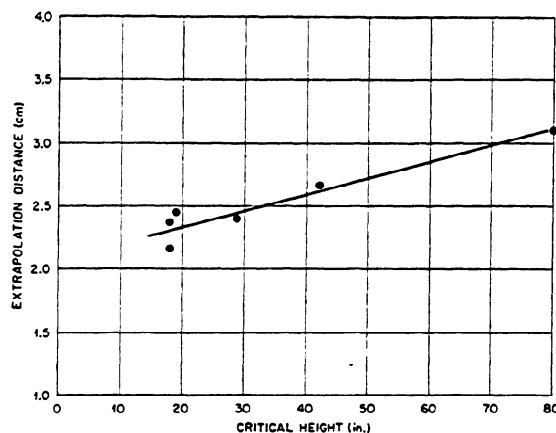


FIG. 3. Extrapolation distances determined with U²³⁵ counter traverses in 60.92-in.-diam cylinder.

fast extrapolation distances experimentally observed was similarly evident in the Corn Pine calculations for the 27.24-in.-diam sphere previously discussed. Within the precision of these experiments the first fundamental theorem of reactor theory is applicable to these systems. The experimental bucklings and their pertinence to the nonleakage probability measurements and calculations are further discussed later in this report.

CROSS SECTIONS

Since the calculated value of the thermal utilization depends upon the absorption cross sections employed, it is appropriate to consider the values used in this report. Safford and Havens (10) have examined the U²³⁵ cross section measurements from various laboratories. The values for the U²³³ cross sections have been tabulated by Evans and Fluharty (11). The g -factors for U²³⁵, used to obtain the Maxwellian-average value of the cross sections from the 2200 meters/sec values, were taken from Westcott and Roy (12). Since the recent tabulation (11) shows the absorption and fission cross section of U²³³ to be $1/v$ in the thermal region, the g -factors for these cross sections must be unity. Table V shows the cross sections used and the appropriate g -factors.

For the fissile isotopes U²³³ and U²³⁵, the resonance integrals given in Table VI were obtained by numerical machine integration of BNL-325 (13, 14) curves.

The following 2200 meters/sec microscopic absorption cross sections, assumed to be proportional to $1/v$, were used for the other components; hydrogen, 0.332 b ; boron, 755 b ; nitrogen, 1.88 b ; thorium, 7.0 b ; U²³⁸, 2.75 b (13); and U²³⁴, 113 b (15); other constituents contributed negligibly.

TABLE V
2200 METERS/SEC CROSS SECTIONS

Isotope	$\sigma_a(b)$	g_a	$\sigma_f(b)$	g_f
U ²³³	573	1.0000	524	1.0000
U ²³⁵	679	0.9749	580	0.9754

TABLE VI
URANIUM RESONANCE INTEGRALS

Resonance integral ^a	U ²³³	U ²³⁵
$\int_{0.2}^{10^6} \frac{\sigma_f}{E} dE, (b)$	930	428
$\int_{0.4}^{10^6} \frac{\sigma_f}{E} dE, (b)$	802	330
$\int_{0.2}^{10^6} \frac{\sigma_t}{E} dE, (b)$	1368	780
$\int_{0.2}^{10^6} \frac{\sigma_a}{E} dE, (b)$	1224	636

^a The absorption resonance integral was calculated on the assumption that the scattering cross section for both isotopes was 11 barns.

FOIL MEASUREMENTS OF THE EPITHERMAL FLUX

The value of λ , given by Eq. (9), was determined experimentally by foil activation measurements. The data from these experiments were corrected for energy dependent flux depression and self-shielding effects.

Trubey (16) has calculated the flux depression and self-shielding coefficient for thermal neutrons in the U²³⁵ metal foils used in these experiments to be 0.79. The flux-weighted average of this factor for the absorptions in the resonances was 0.94. The cross sections used in the calculations have been listed previously in Table V. Attempts were made to measure the order of magnitude of these effects by using foils of different thicknesses and extrapolating to zero thickness. The results of these activations determine a flux depression and foil self-shielding factor, based only on bare activations, of 0.76. This agreement with the calculation may, however, be somewhat fortuitous, considering the nature of the measurements and the approximations in the calculations.

Table VII and Fig. 4 summarize the foil measurements and calculations for the determination of the epithermal flux. The metal and oxide foil measurements, as well as the counter values for both U²³³ and U²³⁵ detectors in both U²³³ and U²³⁵ solutions, are included in these data.

The best-fit line through the data is $\lambda = 0.682 \Sigma_{at}$. From the tabulated values of $\xi \Sigma_t$ for various energies (17), the theoretical expression for λ in infinite systems with no epithermal absorption becomes $0.576 \Sigma_{at}$ at 0.278 ev and has increased to $0.656 \Sigma_{at}$ at 10.16 ev. This higher value is then constant up to the kilovolt energy region. An average value of λ , weighted by the U²³⁵ fission cross section in a $1/E$ spectrum, is $0.63 \Sigma_{at}$. It is realized that λ is a function of the buckling as well as Σ_{at} in a detailed neutron balance theory, but this correction is small and only adds some scatter to the plot of the data in Fig. 4.

EXPERIMENTAL DETERMINATION OF NONLEAKAGE PROBABILITIES

The results from the perturbation measurements of the reactivity as a function of solution height are described in two ways, each emphasizing a particular facet of the theoretical model previously discussed. The leakage parameter, S , defined in Eqs. (22)–(26), depends only on the periods resulting from changes in the height after criticality has been established and on the buckling of the critical system. In Fig. 5 this parameter is plotted as a function of buckling for nine measurements in the 5-ft-diam cylinder with both U²³³ and U²³⁵ solutions and for three measurements in the 9-ft-diam cylinder with U²³⁵ solutions. Experimentally measured extrapolation distances from U²³⁵ counter traverses were used in the calculations to determine bucklings. The curves are theoretical values of S based on the equation and parameters shown in the figure. The values of L^2 were calculated from the relation

$$L^2 = L_0^2(\text{H}_2\text{O}) \frac{\Sigma_a(\text{H}_2\text{O})}{\Sigma_a(\text{Solution})}, \quad (32)$$

in which $L_0^2(\text{H}_2\text{O}) = 7.344 \text{ cm}^2$ (18). For the U²³⁵ solutions the variation of L^2 for variations in B^2 was $L^2 = (3.77 - 106B^2) \text{ cm}^2$ and for U²³³ solutions, $L^2 = (4.14 - 98B^2) \text{ cm}^2$.

Since the fast-neutron extrapolation distances measured with U²³⁵ counters at two critical heights were not significantly different, a constant value, $d = 3.0 \text{ cm}$, was used in a second calculation of the parameter S . These values are plotted as a function of buckling in Fig. 6, and the results of both calculations are summarized in Table VIII. The curves on Fig. 6 show the same theoretical values of S as Fig. 5. As B^2 goes to zero the effect of the extrapolation distance vanishes; thus an extrapolation of

TABLE VII
EXPERIMENTAL DETERMINATION OF λ , THE EPITHERMAL FLUX PARAMETER

Solution			Detector	Detector position in container	Observed cadmium ratio	λ^a
Isotope	Height (in.)	Σ_{at} (cm ⁻¹)				
27.24-in.-diam aluminum sphere						
U ²³⁵	Full	0.05427	U ²³⁵ metal foil	Center	36.50	0.0363
U ²³⁵ + B	Full	0.07723	U ²³⁵ metal foil	Center	27.27	0.0492
U ²³⁵ + B	Full	0.07723	U ²³⁵ metal foil	8 in. from center	26.18	0.0514
U ²³³	Full	0.04743	U ²³⁵ metal foil	Center	39.06	0.0338
U ²³³ + B	Full	0.05523	U ²³⁵ metal foil	Center	36.10	0.0378
48.04-in.-diam aluminum sphere						
U ²³⁵	Full	0.04629	U ²³⁵ metal foil	Center	42.64	0.0309
U ²³⁵	Full	0.04629	U ²³⁵ O ₂ foil	Center	41.55	0.0317
U ²³⁵	Full	0.04629	U ²³⁵ O ₂ foil	Center	16.25	0.0328
U ²³⁵	Full	0.04629	U ²³⁵ metal foil	18 in. from center	40.00	0.0330
U ²³⁵	Full	0.04629	U ²³⁵ counter	Center	49.26	0.0317
U ²³⁵	Full	0.04629	U ²³³ counter	Center	17.08	0.0370
U ²³³	Full	0.04166	U ²³⁵ metal foil	Center	46.08	0.0285
U ²³³	Full	0.04166	U ²³³ O ₂ foil	Center	17.73	0.0299
60.92-in.-diam stainless steel cylinder						
U ²³⁵	17½	0.04975	U ²³⁵ metal foil	Center	39.70	0.0333
U ²³⁵	28	0.04648	U ²³⁵ metal foil	Center	39.67	0.0333
U ²³⁵	41	0.04542	U ²³⁵ metal foil	Center	43.65	0.0302
107.7-in.-diam stainless steel cylinder						
U ²³⁵	35	0.04485	U ²³⁵ metal foil	Center	43.05	0.0306
U ²³⁵	47½	0.04430	U ²³⁵ metal foil	Center	44.88	0.0293
U ²³⁵	95	0.04378	U ²³⁵ metal foil	Center	45.45	0.0289

^a Self-shielding and flux-depression factors of 0.79 for thermal neutrons and 0.94 for epithermal neutrons were used for the foils. These factors were assumed to be unity for the counter data.

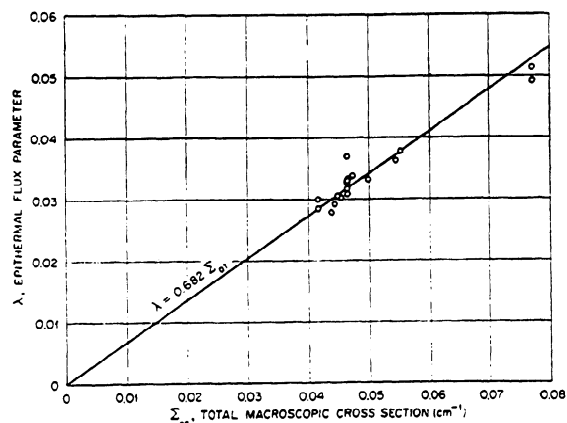


FIG. 4. Epithermal flux parameter

either curve to $B^2 = 0$ should give the same value of M^2 .

Equation (22), in which $P_d(B) = 1/(1 + \tau_d B^2) \cdot (1 + L^2 B^2)$ and $\tau_d = 9 \text{ cm}^2$ (19) was used to evaluate

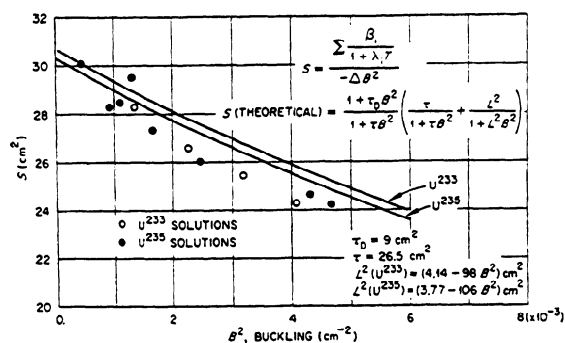


FIG. 5. Leakage parameter variation with buckling determined by the U²³⁵ counter.

the Taylor expansion of $P(B)$. This expansion was given in Eq. (21). The correction term, A , was computed by using the theoretical value of τ , 26.5 cm² (7, 20), and the values of B^2 and L^2 from each experimental determination. From these values of $P(B)$ experimental ages were computed from the

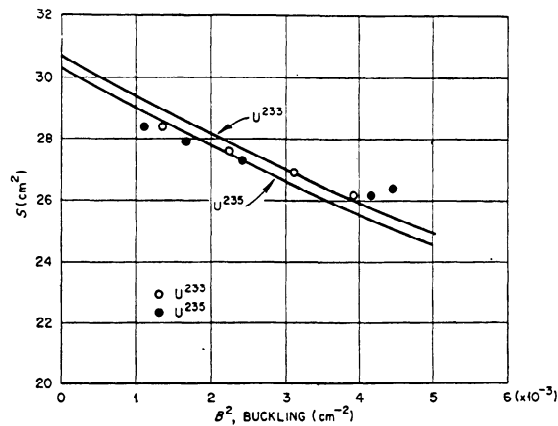


FIG. 6. Leakage parameter variation with buckling determined by using $d = 3.0$ cm.

two-group equation, Eq. (18). Figure 7 plots the experimental age as a function of the buckling determined by the U^{235} counter, while Fig. 8 shows the experimental age as a function of the buckling determined with the fast extrapolation distance.

The average values of the ages of U^{233} and U^{235} fission neutrons to thermal energy derived from the data obtained in the 5-ft-diam cylinder are 25.1 ± 0.5 and 25.8 ± 0.3 cm^2 , respectively, when bucklings are calculated using the thermal extrapolation lengths. The values of the ages are 26.1 ± 0.3 and 26.3 ± 0.3 when bucklings are calculated using the fast extrapolation length of 3.0 cm. Because of buckling uncertainties in the measurements in the 9-ft-diam cylinder described previously, the age

TABLE VIII

SUMMARY OF CALCULATIONS OF THE NONLEAKAGE PROBABILITY AND THE AGE FOR CYLINDRICAL GEOMETRY

Critical ^a height (in.)	Extrapolation ^b distance, d (cm)	Buckling $B^2 \times 10^3$ (cm^{-2})	S (cm^2)	Calculated ^c nonleakage probability	Experimental nonleakage probability	Age to thermal (cm^2)
Cylindrical diam—60.92 in.						
18.31	2.27	4.67 ± 0.11	24.3 ± 0.9	0.8764	0.8814 ± 0.0075	25.1 ± 1.0
	3.00	4.46	26.4	0.8814	0.8759	28.1 ± 1.1
19.20	2.45	4.31 ± 0.10	24.7 ± 0.9	0.8850	0.8880 ± 0.0069	25.6 ± 1.0
	3.00	4.17	26.2	0.8883	0.8854	27.4 ± 1.1
29.23	2.40	2.47 ± 0.05	26.1 ± 0.6	0.9307	0.9340 ± 0.0035	25.0 ± 0.6
	3.00	2.42	27.3	0.9319	0.9321	26.4 ± 0.6
42.06	2.67	1.67 ± 0.03	27.3 ± 0.5	0.9518	0.9534 ± 0.0023	25.5 ± 0.5
	3.00	1.66	27.9	0.9521	0.9528	26.1 ± 0.5
80.68	3.11	1.11 ± 0.02	28.5 ± 0.3	0.9677	0.9680 ± 0.0014	26.1 ± 0.3
	3.00	1.10	28.4	0.9678	0.9683	26.0 ± 0.3
20.02	2.60	4.09 ± 0.10	24.3 ± 0.8	0.8885	0.8967 ± 0.0064	24.0 ± 0.8
	3.00	3.93	26.2	0.8926	0.8927	26.5 ± 0.9
23.85	2.65	3.20 ± 0.07	25.4 ± 0.7	0.9108	0.9160 ± 0.0053	24.6 ± 0.7
	3.00	3.11	26.9	0.9130	0.9132	26.4 ± 0.8
31.12	2.72	2.29 ± 0.05	26.6 ± 0.6	0.9346	0.9378 ± 0.0033	24.9 ± 0.6
	3.00	2.25	27.6	0.9355	0.9362	26.1 ± 0.7
55.18	3.04	1.35 ± 0.03	28.3 ± 0.5	0.9603	0.9612 ± 0.0019	25.8 ± 0.5
	3.00	1.35	28.4	0.9602	0.9610	25.9 ± 0.5
Cylindrical diam—107.7 in.						
35.8		1.31 ± 0.02^d	29.5 ± 0.6	0.9618	0.9606 ± 0.0020	27.5 ± 0.6
47.0		0.93 ± 0.01^d	28.3 ± 0.5	0.9727	0.9734 ± 0.0013	25.7 ± 0.5
94.9		0.44 ± 0.01^d	30.1 ± 0.3	0.9869	0.9867 ± 0.0006	27.0 ± 0.3

^a In the 60.92-in.-diam cylinder critical height values include a correction of 0.53 in. for the bottom structure. In the 107.7-in.-diam cylinder no correction has been included for the effects of structure.

^b Two extrapolation distances and two bucklings are given for each experiment in the 60.92-in.-diam cylinder, the first determined from U^{235} counter flux traverses, the second from U^{238} counter traverses. For the 9-ft-diam cylinder experiments, only U^{235} counter traverses were made to determine the buckling.

^c Calculated from the equation $P(B) = [(1 + \tau B^2)(1 + L^2 B^2)]^{-1}$ with $\tau = 26.5$ cm^2 .

^d Calculated using $B^2 = 0.288 \times 10^{-3}$ and $\bar{h} - h_c$ values of 3.0, 2.0, and 3.5 in. for $h_c = 35.8, 47.0,$ and 94.9 in., respectively. These values are also given in Table IV.

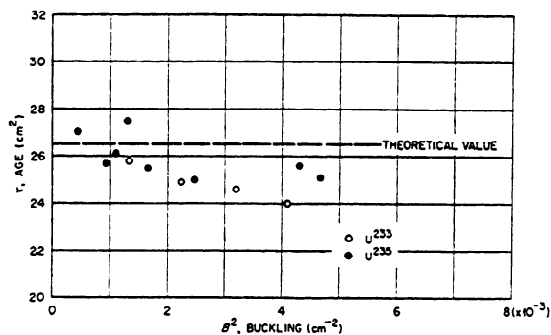
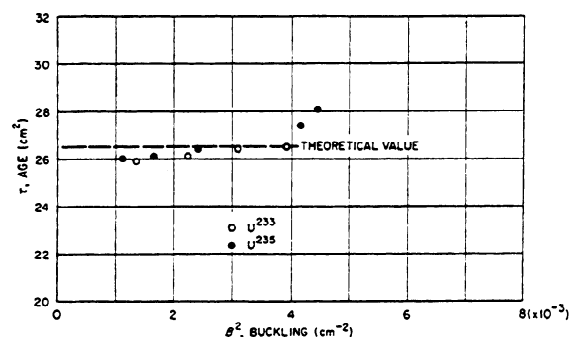
FIG. 7. Age to thermal, using bucklings determined with U²³⁵ counter.

FIG. 8. Age to thermal, using bucklings determined by a constant extrapolation distance.

TABLE IX
EXPERIMENTAL DATA FOR CRITICAL CONDITIONS OF SPHERES

Experiment number	Isotopic composition (wt.%)					Solution density (gm/ml)	Total uranium (mg/gm)	Total boron (mg/gm)	Total nitrate (mg/gm)	Total thorium (mg/gm)	$(k - 1) \times 10^4$ at 20°C
	U ²³³	U ²³⁴	U ²³⁵	U ²³⁶	U ²³⁸						
1	0.00	1.04	93.18	0.27	5.51	1.0288	19.56	0.00	18.7	0.00	11.8
2	0.00	1.04	93.18	0.27	5.51	1.0333	22.77	0.0905	21.2	0.00	7.3
3	0.00	1.04	93.18	0.27	5.51	1.0387	25.77	0.18	23.7	0.00	9.0
4	0.00	1.04	93.18	0.27	5.51	1.0445	27.24	0.22	25.1	0.00	2.8
5	97.70	1.62	0.04	0.00	0.64	1.0226	16.76	0.00	11.9	0.074	5.0
6	97.70	1.62	0.04	0.00	0.64	1.0253	17.42	0.0233	12.3	0.077	10.3
7	97.70	1.62	0.04	0.00	0.64	1.0274	18.03	0.0453	12.8	0.080	10.9
8	97.70	1.62	0.04	0.00	0.64	1.0275	18.67	0.0670	13.2	0.083	3.3
9	97.70	1.62	0.04	0.00	0.64	1.0286	19.27	0.0887	13.6	0.085	4.4
48.04-in.-diam aluminum sphere											
10	0.01	1.05	93.21	0.54	5.19	1.0216	14.82	0.00	11.3	0.00	12.9
11	97.67	1.54	0.03	0.00	0.76	1.0153	13.05	0.00	7.6	0.056	4.6

TABLE X
EXPERIMENTAL DATA FOR CRITICAL CONDITIONS OF CYLINDERS

Experiment number	Critical solution height (in.)	Isotopic composition (wt.%)					Solution density (gm/ml)	Total uranium (mg/gm)	Total nitrate (mg/gm)	Total thorium (mg/gm)
		U ²³³	U ²³⁴	U ²³⁵	U ²³⁶	U ²³⁸				
60.92-in.-diam cylinder										
12	18.31	0.00	1.05	93.22	0.55	5.18	1.0229	16.92	12.8	0.00
13	19.20	0.00	1.03	93.03	0.51	5.43	1.0247	16.61	14.2	0.00
14	29.23	0.00	1.04	93.12	0.54	5.30	1.0209	14.96	12.0	0.00
15	42.06	0.00	1.06	93.11	0.52	5.31	1.0204	14.31	12.2	0.00
16	80.68	0.00	1.06	93.01	0.52	5.41	1.0197	13.79	12.6	0.00
17	20.02	97.37	1.50	0.04	0.00	1.09	1.0203	14.21	8.3	0.014
18	23.85	97.35	1.52	0.05	0.00	1.08	1.0198	13.62	8.6	0.012
19	31.12	97.30	1.49	0.05	0.00	1.16	1.0169	13.00	8.1	0.014
20	55.18	97.25	1.55	0.05	0.00	1.16	1.0166	12.33	8.1	0.098
107.7-in.-diam cylinder										
21	35.8	0.00	1.08	92.79	0.66	5.47	1.0194	14.00	14.2	0.00
22	47.0	0.00	1.06	92.78	0.65	5.51	1.0218	13.66	13.8	0.00
23	94.9	0.00	1.05	92.82	0.63	5.50	1.0210	13.33	13.5	0.00

^a In the 60.92-in.-diam cylinder critical height values include a correction of 0.53 in. for the bottom structure. In the 107.7-in.-diam cylinder no correction has been included for the effects of structure.

determinations in this vessel are not included in the average value of the age for U^{235} fission neutrons. Because of the quoted uncertainty of 4.6% in the absolute yield of delayed neutrons (21), the error in the age must be increased to $\pm 1.3 \text{ cm}^2$. It is concluded that, within the precision of these experiments and accuracy of the delayed neutron fractions, the ages of fission neutrons from U^{233} and U^{235} are the same.

The measured reactivities have been based on delayed neutron data (21) in which the value of ν of U^{235} was taken as 2.47. If a later value of ν , 2.420 ± 0.037 or 2.426 ± 0.068 (22), is used, then the delayed neutron fraction must be increased by 2%. The value of S and the experimental ages calculated from the reactivity measurements would also be increased by this percentage. The value for the age-to-thermal energy becomes $26.6 \pm 1.3 \text{ cm}^2$

for U^{235} fission neutrons in water. It is concluded that these experiments are in agreement with the theoretical values of the age-to-indium resonance energy computed by Coveyou and Sullivan (20), 25.5 cm^2 , and Certain and Aronson (7), 25.7 cm^2 .

CALCULATION OF ETA FROM CRITICAL EXPERIMENTS

The measurement of the nonleakage probability in cylindrical geometry has resulted in confirmation of the theoretical value of the age of fission neutrons to thermal energy. This agreement does not prove that this model can be used for bucklings significantly beyond the range of these experiments. However, such agreement does encourage confidence in the experimental measurements and on the suitability of the model. On this basis, therefore, the sphere comparison measurements have been evaluated also and a value of eta obtained, subject to

TABLE XI
ATOM DENSITIES $\times 10^{-20}$ FOR THE CRITICAL EXPERIMENTS (CM^{-3})

Experiment number	Uranium Isotope					N	H	B	H/X
	U^{233}	U^{234}	U^{235}	U^{236}	U^{238}				
27.24-in.-diam sphere									
1		0.00538	0.48066	0.00138	0.02807	1.869	662.28		1378
2		0.00631	0.56206	0.00163	0.03281	2.129	661.48	0.052	1177
3		0.00716	0.63944	0.00184	0.03734	2.392	660.70	0.104	1033
4		0.00762	0.67959	0.00197	0.03967	2.548	660.28	0.128	972
5	0.43284	0.00716	0.00018		0.00281	1.178	663.60		1533
6	0.45120	0.00744	0.00018		0.00291	1.224	663.45	0.0133	1470
7	0.46798	0.00772	0.00018		0.00301	1.274	663.29	0.0259	1417
8	0.48455	0.00801	0.00021		0.00311	1.319	663.15	0.0383	1368
9	0.50066	0.00827	0.00021		0.00327	1.363	663.00	0.0508	1324
48.04-in.-diam sphere									
10		0.00409	0.36185	0.00220	0.01985	1.116	663.94		1835
11	0.33460	0.00525	0.00010		0.00256	0.753	664.67		1986
60.92-in.-diam cylinder									
12		0.00469	0.41364	0.00243	0.02271	1.272	663.45		1604
13		0.00451	0.40595	0.00222	0.02339	1.409	663.43		1634
14		0.00409	0.36452	0.00209	0.02048	1.185	663.83		1821
15		0.00397	0.34845	0.00194	0.01962	1.208	663.89		1905
16		0.00384	0.33519	0.00186	0.01924	1.244	663.91		1981
17	0.36498	0.00556	0.00019		0.00410	0.826	664.39		1819
18	0.34960	0.00525	0.00018		0.00395	0.849	664.44		1900
19	0.33275	0.00507	0.00017		0.00375	0.802	664.59		1996
20	0.31556	0.00481	0.00016		0.00354	0.795	664.70		2106
107.7-in.-diam cylinder									
21		0.00397	0.33940	0.00240	0.01975	1.407	663.67		1955
22		0.00381	0.33124	0.00232	0.01942	1.367	663.74		2004
23		0.00368	0.32347	0.00220	0.01894	1.338	663.85		2052

the errors in epithermal corrections and in the cross sections. It should be emphasized that the eta ratios obtained from the sphere comparisons are not affected by the errors in the nonleakage probabilities if the ages of fission neutrons are the same for U²³³ and U²³⁵.

All eta values and ratios were calculated with $\tau = 26.5 \text{ cm}^2$ and the thermal and fast bucklings, and each value was assigned a statistical weight proportional to $1/\sigma^2$ in computing the average value. The experimental data are given in Tables IX, X, and XI. The calculations are summarized in Table XII.

The eta ratios, $\bar{\eta}(U^{233})/\bar{\eta}(U^{235})$, deduced from experiments in individual vessels were:

- from 9 experiments in the 27-in.-diam sphere, 1.101;
- from 2 experiments in the 48-in.-diam sphere, 1.103;

from 9 experiments in the 61-in.-diam cylinder, 1.105.

The weighted average thermal values of eta obtained using Eq. (7) are: $\bar{\eta}(U^{233}) = 2.292 \pm 0.015$; $\bar{\eta}(U^{235}) = 2.076 \pm 0.015$. The average value of the ratio $\bar{\eta}(U^{233})/\bar{\eta}(U^{235})$ is 1.104 ± 0.009 . These values of eta and the eta ratio are the same as the 2200 meters/sec values since the g -factors for eta are unity. These results are consistent with the absolute values obtained by Macklin and deSausure (23) using a manganese bath technique. Their values were $\eta(U^{233}) = 2.296 \pm 0.010$, $\eta(U^{235}) = 2.077 \pm 0.010$, and the eta ratio was 1.105 ± 0.007 . The value of the eta ratio should also be compared to 1.116 ± 0.018 , the value obtained by the present authors from a reactivity coefficient experiment (24). The dependence of η upon the absorption cross section of the fissile isotope is given by the relation $\Delta\eta/\eta \approx -0.5\Delta\sigma_a/\sigma_a$.

TABLE XII
CRITICAL EXPERIMENT CALCULATIONS

Experiment number ^a	F	$L^2 \text{ (cm}^2\text{)}$	$B_{th}^2 \times 10^3 \text{ (cm}^{-2}\text{)}$	$P(B_{th})$	$\bar{\eta}(\tau, B_{th})$	$B_F^2 \times 10^3 \text{ (cm}^{-2}\text{)}$	$P(B_F)$	$\bar{\eta}(\tau, B_F)$	
1	0.5867	0.9961	2.999	7.29	0.8202	2.086	6.98	0.8266	2.070
2	0.5852	0.9955	2.557	7.29	0.8228	2.086	6.98	0.8290	2.071
3	0.5824	0.9949	2.237	7.29	0.8247	2.093	6.98	0.8309	2.077
4	0.5830	0.9946	2.107	7.29	0.8254	2.090	6.98	0.8317	2.074
5	0.5262	1.0107	3.431	7.29	0.8177	2.300	6.98	0.8241	2.282
6	0.5256	1.0112	3.287	7.29	0.8185	2.298	6.98	0.8249	2.280
7	0.5246	1.0116	3.164	7.29	0.8192	2.300	6.98	0.8256	2.283
8	0.5238	1.0122	3.045	7.29	0.8199	2.300	6.98	0.8263	2.283
9	0.5228	1.0126	2.947	7.29	0.8205	2.302	6.98	0.8269	2.284
10	0.5178	0.9972	3.515	2.46	0.9308	2.080	2.41	0.9321	2.077
11	0.4627	1.0122	3.906	2.46	0.9300	2.294	2.41	0.9312	2.292
12	0.5508	0.9967	3.271	4.67	0.8764	2.078	4.46	0.8814	2.067
13	0.5459	0.9968	3.304	4.31	0.8850	2.076	4.17	0.8883	2.069
14	0.5195	0.9971	3.501	2.47	0.9307	2.074	2.42	0.9319	2.071
15	0.5082	0.9973	3.583	1.67	0.9518	2.073	1.66	0.9521	2.072
16	0.4985	0.9975	3.653	1.11	0.9677	2.079	1.10	0.9678	2.078
17	0.4843	1.0117	3.746	4.09	0.8885	2.298	3.93	0.8926	2.286
18	0.4736	1.0120	3.825	3.20	0.9108	2.291	3.11	0.9130	2.285
19	0.4614	1.0122	3.915	2.29	0.9346	2.291	2.25	0.9355	2.288
20	0.4482	1.0126	4.012	1.35	0.9603	2.295	1.35	0.9602	2.295
21	0.5013	0.9973	3.628	1.31	0.9618	2.080			2.080 ^b
22	0.4953	0.9974	3.673	0.93	0.9727	2.081			2.081 ^b
23	0.4894	0.9976	3.717	0.44	0.9869	2.076			2.076 ^b
Averages					$\bar{\eta}(U^{233})$	2.294			2.290
					$\bar{\eta}(U^{235})$	2.077			2.075
					$\bar{\eta}(U^{233})/\bar{\eta}(U^{235})$	1.104			1.104

^a See Tables IX and X for identification.

^b This value of η was assumed to be the same as that calculated using the thermal-neutron extrapolation distance since, for this large system, the nonleakage probability and, hence, the calculated η is insensitive to differences in the extrapolation distance.

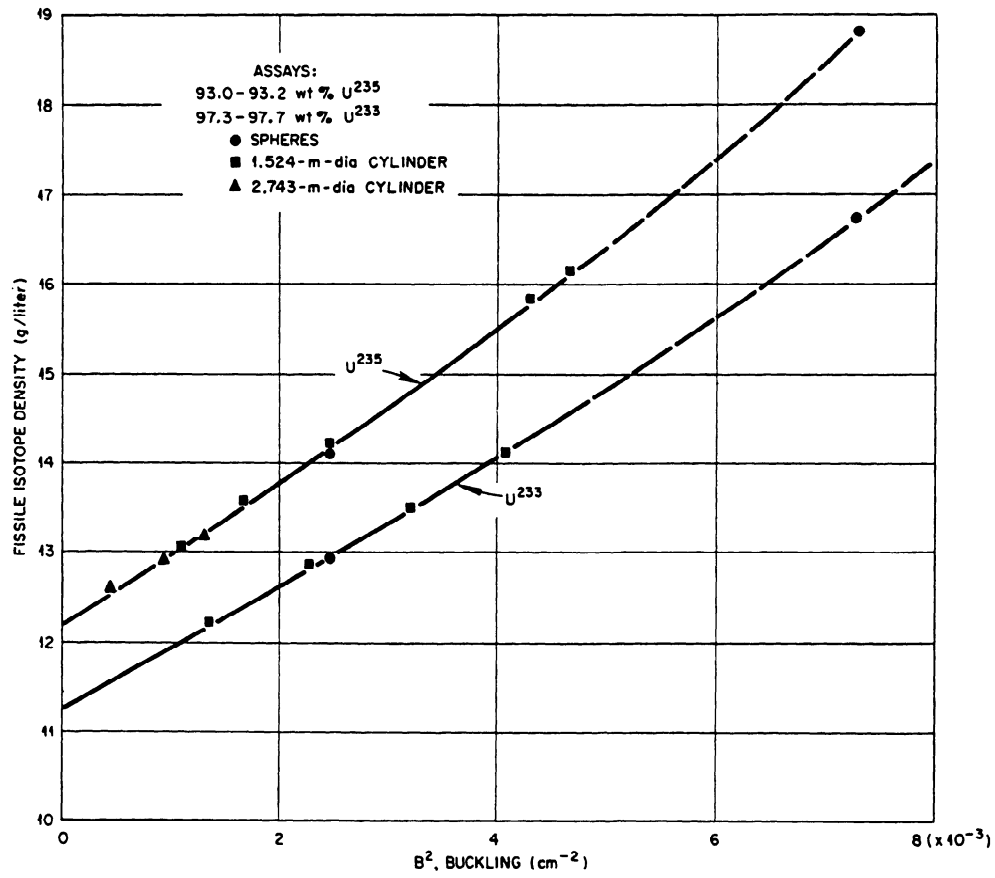


FIG. 9. Fissile isotope densities as a function of buckling in critical aqueous solutions of the nitrates of U²³³ and U²³⁵

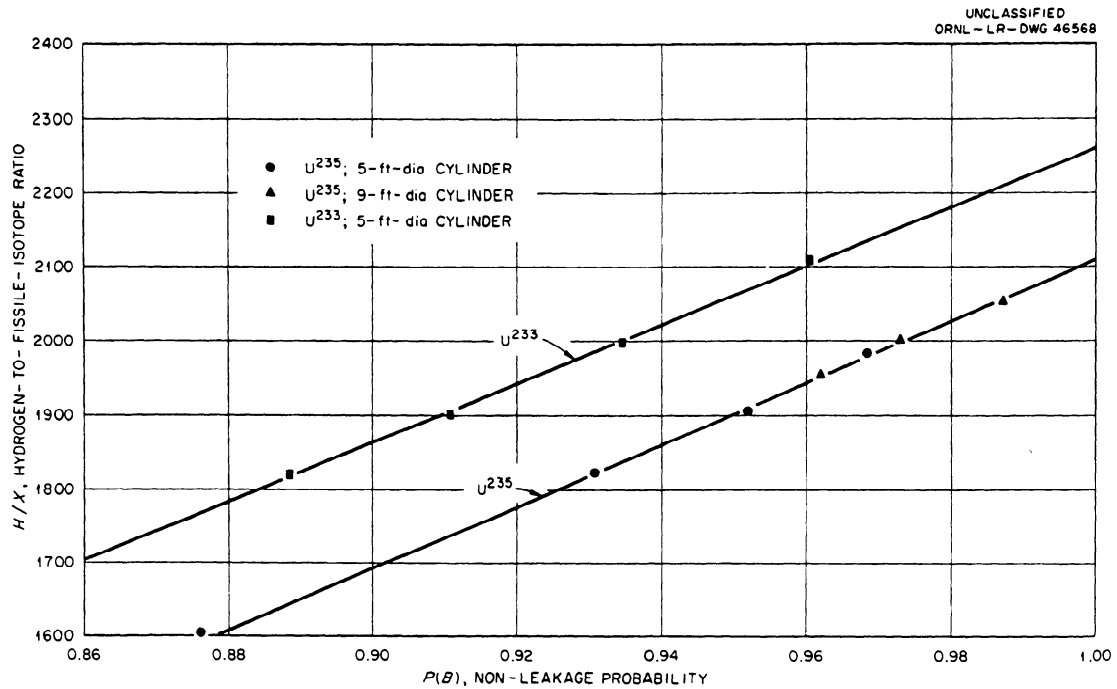


FIG. 10. The hydrogen to fissile isotope ratio as a function of the nonleakage probability

LIMITING CONCENTRATIONS

From the data primarily obtained from the calculation of eta, other information of interest in the fields of reactor physics and nuclear safety can be deduced. If the concentration of the fissile isotope is plotted as a function of the thermal bucklings, an extrapolation to zero buckling can be made. The intercepts are the limiting critical concentrations of U²³³ and U²³⁵ in these nitrate solutions. This plot is shown as Fig. 9. The limiting critical concentrations are 11.25 ± 0.10 gm/liter for the U²³³ solutions and 12.30 ± 0.10 gm/liter for the U²³⁵ solutions.

In addition, if the hydrogen-to-uranium ratio from Table XI is plotted as a function of the non-leakage probability, the result is a straight line. The intercept at $P(B) = 1$ then represents the limiting H/X ratio for each of the nitrate solutions used in these experiments. This plot is shown as Fig. 10. The limiting concentrations for these nitrate solutions are: $H:U^{233} = 2260 \pm 20$ and $H:U^{235} = 2110 \pm 20$. These values of the limiting concentration are in excellent agreement with those calculated using the critical equations, Eq. (7).

ERROR ANALYSIS

The error analysis has been based on the experimental deviations of the measured quantities and the errors on all quantities used in the calculations. The errors quoted are standard deviations. Since the multiplication factor of a critical system can be determined to less than 1×10^{-4} , the errors in the eta values are compounded primarily from non-leakage probability errors and thermal utilization errors.

The errors in the nonleakage probabilities are made up of errors in the leakage parameter, S , and the error of 4.6% in the absolute delayed neutron yield. The errors in the leakage parameter, S , were determined by the observed deviations of reactivities as a function of buckling, B^2 , where buckling errors were derived from the variances in the least squares fit of the counter data from the measured flux traverses.

Thermal utilization errors are dependent upon the macroscopic cross section errors, and range from 0.6% for small systems to 0.7% in the largest systems. These values are compounded from an 0.75% error in the uranium cross sections, an 0.5% error in the uranium density, and an 0.90% error in the hydrogen cross section.

The errors in the epithermal flux and the resonance integrals can be as large as 10% without

introducing more than 0.1% error in the epithermal flux correction factor. Since the epithermal fissions were measured by using the appropriate isotope in the foil measurements, the only source of error in the correction for epithermal absorptions is in the epithermal captures in the uranium isotopes. In other words, the ratio of the fission and absorption integrals might be in error. Because of the size of the epithermal correction factor, F , only 1% different from unity, no error has been included for this term.

ACKNOWLEDGMENTS

The authors acknowledge the participation of J. K. Fox, L. W. Gilley, and D. F. Cronin in the design and performance of the experiments in the 9-ft-diam cylinder. C. Cross and R. K. Reedy provided much technical assistance in these experiments and their precautions during the U²³³ experiments prevented any radioactive contamination. The cooperation of D. K. Trubey, L. Dresner, R. R. Coveyou, and J. G. Sullivan contributed much to the interpretation of the experiments. The authors appreciate the guidance and interest of A. D. Callihan, E. P. Blizard, and A. M. Weinberg throughout these experiments.

REFERENCES

1. W. E. KINNEY, J. G. SULLIVAN, R. R. COVEYOU, AND B. J. GARRICK. Applied Nuclear Physics Division Annual Progress Report ORNL-2081, p. 133 (September 10, 1956).
2. J. T. THOMAS, J. K. FOX, AND A. D. CALLIHAN, *Nuclear Sci. and Eng.* 1, 20 (1956).
3. A. M. WEINBERG AND E. P. WIGNER, "The Physical Theory of Neutron Chain Reactors," p. 381 ff. Univ. of Chicago Press, Chicago, 1958.
4. R. GWIN, A. M. WEINBERG, AND D. K. TRUBEY, *Proc. 2nd Intern. Conf. Peaceful Uses Atomic Energy, Geneva, 1958* 12, 529 (1958).
5. M. J. POOLE, *J. Nuclear Energy* 5, 325 (1957).
6. R. S. STONE AND R. E. SLOVACEK, Neutron spectra measurements. KAPL-1916 (September 1957).
7. J. CERTAINE AND R. ARONSON, Distribution of fission neutrons in H₂O at indium resonance energy. NDA-15-C-40 (June 15, 1954).
8. D. W. MAGNUSON, R. GWIN, AND W. E. KINNEY, Neutron Physics Division Annual Progress Report ORNL-2842, p. 151 (September 1, 1959).
9. D. W. MAGNUSON AND R. GWIN, *Trans. Am. Nuclear Soc.* 2(1), 146 (1959).
10. G. J. SAFFORD AND W. W. HAVENS, JR., Fission parameters for U²³⁵. *Nucleonics* 17(11), 134 (1959).
11. J. E. EVANS AND R. G. FLUHARTY, *Nuclear Sci. and Eng.* 8, 66 (1960).
12. C. H. WESCOTT AND D. A. ROY, Supplement to effective cross section values for well-moderated thermal reactor spectra. CRRP-862 (AECL-869) (August 20, 1959).
13. D. J. HUGHES AND R. B. SCHWARTZ, Neutron cross sections, 2nd ed., BNL-325 (July 1, 1958); D. J. HUGHES,

- B. A. MAGURNO, AND M. K. BRUSSEL, Neutron cross sections, 2nd ed. Suppl. 1 (January 1, 1960).
14. W. E. KINNEY, private communication of Oracle calculations.
 15. J. A. HARVEY, Physics Division Annual Progress Report ORNL-2718 (March 10, 1959).
 16. D. K. TRUBEY, private communication, July 30, 1959.
 17. Reactor physics constants. ANL-5800 (1958).
 18. D. K. TRUBEY, H. S. MORAN, AND A. M. WEINBERG, Appl. Nuclear Phys. Ann. Progr. Rept. ORNL-2389, p. 159 (September 1, 1957).
 19. R. R. COVEYOU AND J. G. SULLIVAN, Neutron Phys. Div. Ann. Progr. Rept. ORNL-2609, p. 82 (September 1, 1958).
 20. R. R. COVEYOU AND J. G. SULLIVAN, unpublished calculations, 1959.
 21. G. R. KEEPIN, T. F. WIMETT, AND R. K. ZEIGLER, *Phys. Rev.* **107**, 1044 (1957).
 22. Recent values by C. J. KENWARD, R. RICHMONDS, J. E. SANDERS, AND B. C. DIVEN *et al.*, quoted by SAFFORD AND HAVENS, *Nucleonics* **17**(11), 134 (1959).
 23. R. L. MACKLIN, G. DESAUSURE, J. D. KINGTON, AND W. S. LYON, *Nuclear Sci. and Eng.* **8**, 210 (1960).
 24. R. GWIN AND D. W. MAGNUSON, Determination of eta by comparison of $\bar{\eta}\sigma_a$ for U^{233} and Pu^{239} with $\bar{\eta}\sigma_a$ for U^{235} in a flux trap critical assembly. *Nuclear Sci. and Eng* **12**, 359 (1962).